

1 **Title: Current Status and Future Strategies for Advancing Functional Circuit Mapping In**  
2 **Vivo**

3 Andre Berndt, Denise Cai, Adam Cohen, Barbara Juarez, Jaume Taura, Hejian Xiong,  
4 Zhenpeng Qin, Lin Tian and Paul A. Slesinger

5  
6 **Abstract:** *The human brain represents one of the most complex biological systems, containing*  
7 *billions of neurons interconnected through trillions of synapses. Inherent to the brain is a*  
8 *biochemical complexity involving ions, signaling molecules, and peptides that regulate neuronal*  
9 *activity and allow for short- and long-term adaptations. Large-scale and non-invasive imaging*  
10 *techniques such as functional Magnetic Resonance Imaging (MRI) and electroencephalography*  
11 *(EEG) have highlighted brain regions involved in specific functions and visualized connections*  
12 *between different brain areas. A major shortcoming, however, is the need for more information*  
13 *on specific cell types and neurotransmitters involved, as well as poor spatial and temporal*  
14 *resolution. Recent technologies have been advanced for neuronal circuit mapping and*  
15 *implemented in behaving model organisms to address this. Here, we highlight strategies for*  
16 *targeting specific neuronal subtypes, identifying, and releasing signaling molecules, controlling*  
17 *gene expression, and monitoring neuronal circuits in real-time in vivo. Combined, these*  
18 *approaches allow us to establish direct causal links from genes and molecules to the systems*  
19 *level and ultimately to cognitive processes.*

20  
21 Recent advances in deconstructing neuronal circuits *in vivo* involve the synergy of four  
22 areas: cell-specific expression of proteins using molecular genetics, monitoring neuronal activity  
23 and neuromodulators over time, triggering the release of specific transmitters, and tracking  
24 behaviors. Using model organisms like rodents allows one to target distinct cell types with  
25 protein-based tools such as fluorescent proteins and light-activated ion channels. Viruses  
26 encoding these tools are injected into the brain, and their expression is restricted to specific cell  
27 types under the control of Cre or Flp recombinase in transgenic rodent driver lines (Gong et al.,  
28 2007; Weinholtz and Castle, 2021). For example, tracing experiments label distinct neuronal  
29 subtypes with fluorescent proteins, allowing axonal projections to be traced by various  
30 volumetric imaging techniques (Oh et al., 2014; Glaser et al., 2023). This type of circuit mapping  
31 can scale to subcellular levels and reveal intricate anatomical features, such as dendritic and  
32 axonal arborization, identifying convergent or divergent connections from one brain region to  
33 another.

34 While these imaging techniques provide details on the connectome, they lack dynamic  
35 information on activity or the biological compounds that regulate these signals. Recent  
36 advances in sensor engineering and caging of neuromodulators enable us to monitor intra- and  
37 extracellular signaling molecules with high spatial and temporal resolution in head-fixed or even  
38 freely moving animals. For example, genetically encoded fluorescent sensor proteins can  
39 monitor calcium, voltage, dynorphin, dopamine, norepinephrine, acetylcholine, orexin, and more  
40 (Patriarchi et al., 2018; Adam et al., 2019; Feng et al., 2019; Jing et al., 2020; Abraham et al.,  
41 2021; Duffet et al., 2022; Zhang et al., 2023).

42 Concurrently, several imaging techniques have been developed to monitor these  
43 sensors. Miniaturized fluorescence microscopes are head-mounted onto freely moving rodents  
44 for *in vivo* detection (Ghosh et al., 2011; Cai et al., 2016). Two-photon microscopy through  
45 transcranial windows of head-fixed animals provides sub-cellular resolution. It can be  
46 complemented by Gradient Refractive Index (GRIN) lenses or prisms to image deep brain areas  
47 (Levene et al., 2004; Andermann et al., 2013). Fiber photometry detects bulk fluorescence  
48 through implanted optical fibers, targeting specific neuronal subpopulations and analytes (e.g.,  
49 voltage,  $Ca^{2+}$ , neurotransmitters, neuromodulators) (Gunaydin et al., 2014) These tools allow for  
50 a distinct assessment of the roles of cell types, neuronal circuits, neurotransmitters, and  
51 neuromodulators in cognitive functions. For example, they revealed the dynamics of dopamine

52 release from the ventral tegmental area during reward paradigms, the firing-dependent  
53 volumetric release of acetylcholine in the entorhinal cortex, and orexin dynamics in  
54 somatosensory cortex and basal forebrain during wake-sleep cycles (Patriarchi et al., 2018; Jing  
55 et al., 2020; Duffet et al., 2022).

56 Optogenetic (Yizhar et al., 2011) and chemogenetic (Vardy et al., 2015) actuators, such  
57 as channelrhodopsins and DREADDS, link circuits to behaviors by directly manipulating  
58 neuronal activity. Membrane potentials can be depolarized or hyperpolarized, and light-activated  
59 ion channels can trigger neurotransmitter release. Intracellular signaling cascades can be  
60 modulated by designer G-protein coupled receptors (GPCRs) such as DREADDs, by light-  
61 activated adenylyl cyclases such as bPAC (Stierl et al., 2011) or light-activated GPCRs such as  
62 parapinopsin (Copits et al., 2021) and OPN3 (Mahn et al., 2021). Combining these techniques  
63 allows simultaneous monitoring and manipulation of targeted neuronal circuits. For instance,  
64 one can trigger neuromodulator release from a specific cell type using channelrhodopsin and  
65 simultaneously monitor the activity of connected downstream neurons using calcium imaging or  
66 sensors for neuromodulators. This combined approach enables the reconstruction of detailed  
67 cellular and molecular maps of brain circuitry and informs our understanding of the interplay  
68 between brain regions during cognitive processes.

69 The past 15 years saw tremendous progress in functional circuit mapping in model  
70 organisms. In the context of fear memory, specific groups of neurons (known as engram cells)  
71 in the entorhinal cortex and within various regions of the hippocampus are thought to encode  
72 contextual information. In contrast, engram cells in the amygdala primarily encode fear-  
73 associated information. A series of mapping experiments revealed that these distinct cell  
74 ensembles form a complex network encapsulating the fear memory (Josselyn and Tonegawa,  
75 2020). Similarly, *in vivo* calcium imaging of the CA1 region in the hippocampus of freely moving  
76 rats visualized and tracked hundreds of place cells, crucial for spatial navigation and memory,  
77 over weeks. This innovative approach revealed that place cells could maintain their location  
78 specificity over extended periods, providing insights into hippocampal circuit organization, which  
79 is vital for memory, navigation, and learning (Wirtshafter and Disterhoft, 2022).

80 Other mapping studies have shown the importance of mPFC's dopaminergic afferent  
81 connection with the ventral tegmental area (VTA) in managing social avoidance and stress  
82 resilience. Furthermore, efferent connections from mPFC to other regions like the basolateral  
83 amygdala (BLA) were critical in reversing stress-induced behavioral deficits and producing rapid  
84 antidepressant effects. Manipulation of the mPFC's various circuits influenced anxiety and  
85 depression-like behaviors, indicating the central role mPFC plays in regulating affective states  
86 (Liu et al., 2021).

87 Another study monitored thousands of striatal spiny projection neurons of the direct  
88 (dSPNs) and indirect (iSPNs) pathways in the basal ganglia. The results showed that L-DOPA  
89 can cause imbalances in the basal ganglia when treating Parkinson's due to the differential  
90 responses of dSPN and iSPN pathways. Thus, future treatments need to consider the activity  
91 rates and the spatial-temporal coordination of neurons within these circuits (Parker et al., 2018).

92 These examples show that the future of circuit mapping relies on increasingly precise  
93 and multifaceted methods matching the complexity of brain circuits. This review highlights  
94 recent technological advances in 1. genetically encoded sensors, 2. recording neuronal activity  
95 with mini-microscopes, 3. protein integrators of neuronal activity, 4. CRISPR/Cas9 gene editing,  
96 and 5. time-locked release of neuropeptides from nanovesicles (Fig. 1). These topics were  
97 discussed at a corresponding symposium at the 2023 annual meeting of the Society for  
98 Neuroscience.

99

100 **Next generation sensor design: Overcoming challenges in protein engineering.**  
101 One key to circuit mapping is monitoring the release of neuromodulators and neuropeptides  
102 from genetically defined neuron populations. Fluorescent sensor proteins are ideally suited for

103 this task because they can be engineered to bind specific ligands, and their expression can be  
104 spatially restricted by Cre-Lox recombination or cell-specific promoters. Existing sensors for  
105 calcium and neurotransmitters have provided new information on neuronal circuits. However,  
106 much work remains to improve the brightness, sensitivity, kinetics, dynamic range, spectral  
107 tuning, and specificity of sensor proteins. For example, *in vivo* imaging of individual neurons  
108 through transcranial windows or miniaturized microscopes requires highly optimized sensors  
109 with large signal amplitudes. For imaging neuronal activity through calcium transients, this  
110 threshold was initially reached with the development of GCaMP6 from GCaMP3 (Chen et al.,  
111 2013).

112 In addition, there is a vast array of targets for future sensor development. Here, we  
113 consider the family of opioid receptors and peptides. Despite the large body of research on  
114 opioid receptor function, there is a limited understanding of the endogenous opioid peptides  
115 released in neuronal circuits. Fluorescent opioid sensors could identify the specific types of  
116 neurons that release endogenous opioids during pain responses, reward, or stress. One  
117 example is the recently developed sensor kLight1.2, based on the kappa-opioid receptor. The  
118 sensor could detect dynorphin release in the medial prefrontal cortex of mice under morphine  
119 withdrawal (Abraham et al., 2021). A similar prototype sensor based on the mu-opioid receptor,  
120 however, failed to generate a sufficient signal response, highlighting the need for further  
121 optimization (Patriarchi et al., 2018).

122 Optimizing fluorescent sensors for detecting neuropeptides via mutagenesis has been a  
123 significant challenge due to the immense mutational landscape of proteins. Targeting only five  
124 residues by randomized mutations can result in 3.2 million variants. This number far exceeds  
125 the current throughput of screening approaches for most sensor proteins (usually in the low  
126 hundreds). Newly developed high-throughput systems such as BeadScan (Koveal et al., 2022)  
127 and Opto-MASS (Rappleye et al., 2022) and video-based pooled screens (Tian et al., 2023) can  
128 functionally test signal amplitudes, kinetics, and ligand selectivity of semi-randomly mutated  
129 variants in minutes. For example, Opto-Mass tested 21,000 variants of mLight and identified a  
130 significantly improved variant called uMASS, which features improved membrane trafficking as  
131 well as five times larger response amplitudes towards the synthetic opioid [D-Ala<sup>2</sup>, N-MePhe<sup>4</sup>,  
132 Gly-ol]-enkephalin (DAMGO).

133 uMASS inherits the ligand binding promiscuity of the mu-receptor. Accordingly, it is  
134 highly sensitive to Met-enkephalin but also detects endorphin, Leu-enkephalin, and dynorphin  
135 with lower affinities. Future opioid sensors for each type would allow us to distinguish neurons  
136 producing different opioids. Given that different opioids can have complementary or opposing  
137 effects, multiple opioid-specific fluorescent sensors could uncover competitive receptor binding  
138 or the co-release of opioids. High-throughput screening platforms such as Opto-MASS can be  
139 adapted to screen sensor libraries while several competing agonists are applied sequentially.  
140 The screen could identify variants with distinct selectivity profiles, such as high met-enkephalin  
141 and low endorphin affinity or vice versa.

142 These high-throughput approaches create large datasets that link mutations to sensor  
143 functions. Implementing machine learning (ML) to these datasets could significantly advance  
144 sensor engineering. In one recent example, ~1,000 mutations of GCaMP were used to train ML  
145 ensembles to predict response amplitudes and kinetics of known GCaMP mutations (Wait et al.,  
146 2023). The final ML ensembles incorporated the five amino acid properties out of 554, with the  
147 highest predictive power for the function of GCaMP variants. The ML model was applied to a  
148 library of 1,423 previously untested GCaMP mutants. Variants with high fluorescence and  
149 kinetic responses were subsequently tested. Two variants, called ensemble-GCaMPs  
150 (eGCaMP+ and eGCaMP2+), have generated the largest dynamic range of any calcium  
151 indicator, while eGCaMP+ is also the fastest known variant in these tests (Wait et al., 2023).

152 These ML models can be applied to map sequence-function relationships in new  
153 sensors instead of more complex structure-function relationships. These approaches will

154 become invaluable to significantly accelerate sensor engineering when combined with high-  
155 throughput platforms. Such next-generation methods are urgently needed: ~6,000  
156 neuropeptides have been discovered in vertebrate and invertebrate organisms, with most  
157 functions only weakly defined at the circuit level (Wang et al., 2015). Beyond neurotransmitters  
158 and neuromodulators, sensors that detect changes in neurotrophic factors, such as BDNF  
159 (Brain-Derived Neurotrophic Factor), could provide insights into neural development, neural  
160 plasticity, and neurodegenerative processes. A sensor for cortisol could help us better  
161 understand the brain's response to stress. Furthermore, developing sensors to detect signaling  
162 molecules involved in immune responses, like cytokines, could be revolutionary. Traditional  
163 (slow) trial-and-error mutagenesis for engineering and optimizing these sensors would require  
164 tremendous resources and time commitments. Further advances in protein engineering are  
165 critical to overcome these challenges (Fig. 2).

166

### 167 **Functional Imaging of neuronal circuits in freely moving rodents with Miniscopes**

168 While monitoring the release of neuromodulators in real time using sensors provides information  
169 on when and where these molecules are released, it is also essential to study the effect on the  
170 activity of individual neurons. One of the most frequently used fluorescent sensors is GCaMP for  
171 measuring changes in intracellular calcium, which occurs downstream of action potentials. Due  
172 to the slower time scales of calcium sensor kinetics compared to voltage sensor kinetics,  
173 imaging acquisition rates are lower than for voltage indicators and allow lower excitation light  
174 power, reducing hardware demands and photobleaching. Combining fluorescent biosensors  
175 with miniaturized microscopes using gradient refractive index (GRIN) lenses instead of  
176 traditional objective lenses enables probing deeper brain regions like the hippocampus,  
177 thalamus, striatum, orbitofrontal cortex, and brainstem. Microscope miniaturization can be  
178 combined with robust behavioral paradigms to allow the investigation of circuits underlying  
179 functions such as learning and memory (Ghosh et al., 2011; Cai et al., 2016).

180 The use and development of the open-source UCLA Miniscope is one example of how *in*  
181 *vivo* imaging can be applied to answer complex questions about memory dynamics *in vivo*. For  
182 instance, Miniscopes recorded active neurons as mice explored varying contexts (Fig. 3). These  
183 tests proved that memories that occur within a day are more likely to share an overlapping  
184 neural ensemble, leading to behavioral linking: the recall of one memory likely triggers recall of  
185 the other memory that occurred close in time. Additionally, specific memory-linking deficits in  
186 aged mice were rescued using artificial ensemble activation via chemogenetic stimulation by  
187 DREADDS (Vardy et al., 2015). These experiments provided novel and critical insight into how  
188 the brain organizes and integrates different experiences across time. A future question is how  
189 memories are encoded across even longer time scales. A recent preprint details how strong  
190 aversive experiences drive ensemble reactivation of a neutral memory formed two days prior,  
191 effectively transferring fear from the aversive to the neutral context (Zaki et al., 2023). Such  
192 findings indicate that memory linking can occur between events rather than only at initial  
193 memory encoding, suggesting a mechanism that allows the brain to associate memories across  
194 time.

195 There is a need to increase access to these powerful imaging technologies, as  
196 evidenced by the growing number of users involved in the UCLA Miniscope project. To remove  
197 barriers to technology adoption and iteration, all aspects of the Miniscope—from the hardware  
198 components to the software used for analysis—were selected based on their widespread  
199 availability. The success of the UCLA Miniscope project has prompted the initiation of many  
200 others, including NINscope (de Groot et al., 2020), cScope (Scott et al., 2018), MiniFAST  
201 (Juneau et al., 2020), Miniscope3D (Yanny et al., 2020), and Mesoscope (Rynes et al., 2021).  
202 These collective efforts have engendered innovative approaches that leverage 3D imaging,  
203 variable sampling rates, and different fields of view.

204 Though powerful in providing anatomically precise, circuit-level investigations of brain  
205 function, existing tools have limitations. Miniscope designs generally use a one-photon wide  
206 field image similar to a tabletop fluorescent microscope and produce images that are projections  
207 from the distal tip of the GRIN lens. These one-photon imaging approaches are prone to out-of-  
208 focus light from other depth planes scattering and producing noise in the field of view. Image  
209 analysis requires spatiotemporal unmixing of the 2D images to differentiate cells and separate  
210 signal from noise. While the currently used algorithms can extract calcium activities from  
211 individual neurons fairly reliably amidst high noise levels, ensuring that the same neuronal  
212 populations are recorded across imaging sessions remains challenging. Due to the chromatic  
213 aberration of GRIN lenses that are typically used in Miniscope, Miniscopes are typically only  
214 able to record one wavelength of light at a time, precluding the possibility of recording multiple  
215 fluorophores simultaneously in the same field of view. In contrast, two-photon microscope  
216 systems can measure multiple signals simultaneously and do not suffer from contamination by  
217 out-of-focus light scattering; however, their requirement for head-fixed preparations hinders use  
218 in many behavioral paradigms.

219 To overcome these limitations, there are continual developments in open-source single-  
220 photon and two-photon Miniscopes with multiwavelength recording capabilities (Zong et al.,  
221 2021)(Zong et al., 2022). This allows for simultaneous imaging of two dynamic signals, such as  
222 dopamine and calcium, using dLight (Patriarchi et al., 2018) and GCaMP (Chen et al., 2013) or  
223 a static signal with a dynamic signal (e.g., tagging cells with constitutively active indicators like  
224 tdTomato and monitoring changes with GCaMP). Innovative software, such as CalmAn  
225 (Giovannucci et al., 2019) and Minian (Dong et al., 2022), for calcium imaging analysis, have  
226 been developed to be combined with programs like DeepLabCut (Mathis et al., 2018) relating  
227 behavioral responses to neuronal activity. As these approaches allow researchers to modulate  
228 and monitor neuronal signaling in behaving animals with high spatial and temporal resolution, it  
229 is critical to continue promoting affordable and user-friendly implementation as new  
230 technologies develop.

### 231 **Integrators and Tickertapes for imaging brain-wide neuronal activity**

232 In parallel with the development of new sensors and imaging systems is the search for  
233 techniques to monitor the activity of an unlimited number of individual neurons that can be  
234 recorded simultaneously. With current imaging techniques, light scatter constrains live-tissue  
235 imaging to depths of typically < 500 nm for two-photon microscopy and < 1 mm for three-  
236 photon. Efforts to image deeper require the destruction of overlying tissue and sometimes  
237 sacrificing single-cell resolution. On the other hand, brain-wide maps of macromolecular signals  
238 (e.g. gene expression or protein levels) can be generated in fixed tissues. Still, these maps  
239 probe only a single point in time and do not capture physiological signals such as calcium or  
240 neuromodulators (**Fig. 4A**). Thus, neuroscientists face a tradeoff between dynamical and spatial  
241 information.

242 Several recently developed techniques show a path toward transcending this tradeoff.  
243 The key feature is to create long-lived chemical traces that record transient events within  
244 individual cells. The encoding occurs *in vivo*, but the readout is measured *ex vivo*. While whole-  
245 brain recordings are not yet possible, there are exciting advances in several areas.

246 First, light-gated integrators store a snapshot of neural activity in a long-lived chemical  
247 signal (Fig. 4B). As their name suggests, these tools build up a signal proportional to the  
248 cumulative activity during an interval defined by a light pulse. In one technique, a light-gated  
249 voltage integrator and a light-gated voltage sample-and-hold reporter store long-term records of  
250 electrical activity via the conformation of a microbial rhodopsin (Venkatachalam et al., 2014).  
251 Alternatively, a light-gated calcium integrator, CaMPARI, undergoes an irreversible green-to-red  
252 transition in the simultaneous presence of calcium and violet light (Fosque et al., 2015). These

254 tools enable *ex vivo* mapping of circuits that had been active during the illumination epoch.  
255 However, they do not provide any downstream genetic access to these cells.

256 The ST-Cal-Light (Lee et al., 2017b; Hyun et al., 2022), FLiCRE (Kim et al., 2020), and  
257 scFLARE2 (Sanchez et al., 2020) light-gated calcium integrators also sense cumulative calcium  
258 during an optically gated interval. These tools also provide a transcriptional readout (Fig. 4C).  
259 With these tools, a transcription factor is tethered to the cell membrane by a linker cleaved in  
260 the simultaneous presence of blue light and calcium. FLiCRE requires three genetic  
261 components (two for the integrator and one for the readout). The scFLARE2 integrator has a  
262 single sensing component (but still requires another gene as the readout). This approach  
263 allows the coupling of the  $\text{Ca}^{2+}$  activity signal to a wide range of subsequent measurements or  
264 perturbations. For instance, an optogenetic actuator or silencer could be expressed to test the  
265 causal roles of the tagged neurons. Alternatively, structural markers could be expressed to  
266 assess their connectomes or ribosome pulldown tags to measure their ensembles of translated  
267 proteins.

268 SPARK (Kim et al., 2017) and iTANGO (Lee et al., 2017a) reporters operate on a similar  
269 principle to FLiCRE and scFLARE but are sensitive to the activation of G-protein coupled  
270 receptors (GPCRs). These reporters have a modular design so that they can be coupled to  
271 various upstream receptors, as well as arbitrary transcriptional readouts. Integrators have been  
272 developed for dopamine receptors D1 and D2, the beta-adrenergic receptor, and others.

273 Existing light-gated integrators have two key limitations. First, these tools only provide a  
274 single readout. Ideally, one wishes to map changes in signal associated with a particular  
275 experimental condition, but the existing tools can be confounded by basal activity unrelated to  
276 the experiment. Readouts at multiple times would also permit comparison of patterns of neural  
277 activation under different conditions within the same animal. Second, existing integrators  
278 require blue or violet light for the optical gate. Due to strong blue light scattering in tissue, this  
279 limits the recording depth to  $\sim 1$  mm. In principle, red or infrared-gated integrators could record  
280 throughout a mouse brain, with light sources mounted outside the skull.

281 Several recent efforts have sought to provide multi-time-point measures of neural activity  
282 and to overcome the depth limitations of light-gated integrators. Protein tickertapes comprise  
283 linearly growing protein fibers that incorporate colored bands during epochs of neural activity,  
284 which are then read *ex vivo*. Based on linear crystals of the Pak4 kinase, one approach has an  
285 absolute time resolution of  $\sim 30$  minutes, but the crystals deform the cells and thus are  
286 incompatible with *in vivo* use (Fig. 3D) (Lin et al., 2023). Another approach is based on  
287 filaments of *E. coli* isoaspartyl dipeptidase but has a time resolution of days and does not have  
288 an absolute time-base (Mohar et al., 2022). In both cases, expression of the tags is driven by  
289 neural activity-dependent genes (e.g. cfos), which are downstream of action potentials.

290 Pulse-chase labeling with HaloTag-ligand dyes also provides a means to capture  
291 aspects of neural activity at multiple time points. In one recently demonstrated technique,  
292 dubbed DELTA, protein turnover was mapped brain-wide via pulse-chase labeling of HaloTag-  
293 protein fusions with multiple colors of brain-permeant HaloTag-ligand dyes. In another  
294 technique, dubbed EPSILON, newly surface-exposed AMPA receptors were identified via pulse-  
295 chase labeling with multiple colors of membrane-impermeable dyes (Kim et al., 2023).  
296 EPSILON could identify synapses potentiated during a particular chemically gated window *in*  
297 *vivo*, providing an approach to mapping the physical basis of memory formation.

298 The field of light- and chemical-gated integrators and tickertapes is still in its infancy.  
299 Nonetheless, these tools promise to provide a view that complements existing *in vivo* and *ex*  
300 *vivo* tools for functional circuit mapping, revealing brain-wide maps of multiple chemical signals  
301 as a function of time.

302 **303 CRISPR/Cas9 gene editing approaches to study gene function**

304 While genetically encoded fluorescent sensors can be targeted to specific types of  
305 neurons using specific promoters and Cre-lines of mice, it is also essential to determine the  
306 causal roles of specific genes in neural circuit dynamics. The basis for the functional,  
307 anatomical, and molecular diversity in the brain is fundamentally linked to the gene expression  
308 diversity of cells within neuronal circuits. Consequently, gene editing technologies such as  
309 CRISPR-Cas9, which modify gene expression, are critical for complementing the connectome  
310 with genetic information (Charpentier and Marraffini, 2014; Heidenreich and Zhang, 2016).  
311 Combined with neurophysiological tools and behavioral analyses, gene-editing technologies will  
312 provide new insights into the genetic basis of brain function (Savell and Day, 2017).

313 Gene-modifying approaches such as knock-in and knock-out transgenic mice, virally  
314 mediated gene delivery of RNA interference (RNAi) constructs, targeting of DNA nucleases,  
315 including zinc-finger nucleases (ZFNs) and transcription activator effector nucleases (TALENs),  
316 have helped to discover new genetic contributions to brain function (Urnov et al., 2005; Limaye  
317 et al., 2009; Wang et al., 2013). Yet, the high costs, time for generation, temporal limitations,  
318 and complexity of some of these methods restrain their application. Recently, using CRISPR  
319 technology combined with Cas bacterial enzymes like Cas9 has addressed many shortcomings  
320 of earlier methods.

321 CRISPR-Cas9-based gene-editing approaches engineered for eukaryotic systems are  
322 based on the guidance of Cas9 nucleases to a DNA target site of interest using single-guide  
323 RNAs (sgRNAs) (Jiang and Doudna, 2017; Kalamakis and Platt, 2023). Once the sgRNAs  
324 deliver Cas9 to the site of interest in DNA, the DNA is unwound and cleaved near a protospacer  
325 adjacent motif (PAM) (**Fig. 4A**). Cellular mechanisms of either homology-directed repair (HDR)  
326 or non-homologous end joining (NHEJ) are recruited to repair the double-stranded break (DSB)  
327 in the DNA (Day, 2019). HDR pathways are usually recruited in dividing cells and use DNA  
328 template strands to precisely edit and repair the DSBs. In non-dividing cells (like neurons),  
329 NHEJ mechanisms are instead usually recruited, resulting in random insertions, deletions, or  
330 base-pair substitutions to correct the DSB, thus disrupting gene expression.

331 In addition, catalytically inactive (“dead”) Cas9 (dCas9) is altered to prevent DNA  
332 cleavage while retaining sgRNA-directed guidance. Thus, dCas9 can guide fused effector  
333 proteins to specific DNA sequences (**Fig. 4B**) (Gilbert et al., 2013). These approaches have  
334 been further expanded by CRISPR interference (CRISPRi) to repress gene transcription and  
335 CRISPR activation (CRISPRa) that can activate transcriptional states (Pickar-Oliver and  
336 Gersbach, 2019; Savell et al., 2019; Duke et al., 2020). Recently, CRISPR/Cas9 systems have  
337 been used to shuttle other epigenetic effector proteins to alter gene expression (Choudhury et  
338 al., 2016; Choi et al., 2023).

339 Applying these CRISPR-Cas9 approaches *in vivo* has expanded our knowledge of  
340 genetic contributions to brain function. For example, two adeno-associated virus (AAV)-  
341 mediated gene delivery can express the CRISPR/Cas9 system in the adult mouse brain  
342 knocking out genes of interest (Swiech et al., 2015). The development of *Cre*-inducible Cas9  
343 knock-in mice further revolutionized genome editing and its application across systems (Platt et  
344 al., 2014). It allowed crossing these mice with *Cre*-driver lines to specifically express Cas9 in  
345 cell types of interest in the nervous system. Thus, by virally delivering sgRNAs into targeted  
346 brain regions, it can induce rapid genome alterations in a cell-type specific manner (Yamaguchi  
347 et al., 2018; McQuillan et al., 2022).

348 In 2020, a conditional, single AAV-based approach was used to express a smaller Cas9  
349 and sgRNAs in adult mammals (Hunker et al., 2020). The resulting gene mutagenesis was as  
350 efficient as gene disruption in knockout mice. Juarez *et al.* recently combined these approaches  
351 with *in vivo* opto-electrophysiology, fiber photometry, and two-photon slice imaging to elucidate  
352 how ion channels contribute to patterns of VTA physiology and reinforcement learning (Juarez  
353 et al., 2023). Notably, the conditional, single-AAV-based method could be combined with *Cre*-  
354 recombinase or *Flp*-recombinase systems. A compelling finding of this study was that neurons

355 in the lateral hypothalamus produce both stimulating neuropeptides and inhibitory GABA ( $\gamma$ -  
356 aminobutyric acid). Notably, these signals are used in a coordinated manner to control neurons  
357 in the VTA that regulate dopamine release (Soden et al., 2023).

358 Advances in CRISPR-Cas9 approaches are now opening the door for ways to  
359 manipulate the genome of adult animals to better model human conditions (Cox et al., 2015).  
360 Methods that shift the DSB repair mechanism from NHEJ to HDR are being refined to introduce  
361 single nucleotide polymorphisms (SNPs) in the adult nervous system (Scholefield and Harrison,  
362 2021). This could broaden the application of CRISPR to activate or repress genes of interest  
363 and model human disease-associated SNPs in animals. A critical feature for future applications  
364 is the temporal control of CRISPR-Cas9 function, which is under development and includes  
365 optogenetic or pharmacological induction of gene editing (Savell and Day, 2017; Choi et al.,  
366 2023).

367

### 368 **Photosensitive Nanovesicles: A Promising Tool for Precise Neuromodulation**

369 A missing tool in the arsenal of measuring the release of neuromodulators, studying the  
370 activity on neurons, and mapping brain-wide circuits is the ability to control the release of a  
371 specific neurotransmitter or neuromodulators within a targeted brain region. Recent advances  
372 have improved the ability for spatially and temporally precise delivery of neuro-active  
373 compounds.

374 It is now possible to remotely control the release of neuroactive compounds using external  
375 stimuli such as magnetic fields (Rao et al., 2019), ultrasound (Airan et al., 2017; Wang et al.,  
376 2018), or light (Rapp and DeForest, 2021). Among these methods, light-based modulation  
377 offers high temporal and spatial resolution. One approach is to cage a desired neuroactive  
378 molecule by blocking a group key for its biological activity, where the molecule remains inactive  
379 until photo-uncaging (Ellis-Davies, 2007; Taura et al., 2018). While various caged compounds  
380 exist, such as glutamate or GABA (Ellis-Davies, 2020), their use is limited by residual activity,  
381 low solubility, and uncaging efficiency (Silva et al., 2019), and the risk of off-target effects (Maier  
382 et al., 2005; Noguchi et al., 2011). Along the same line, studying the role of neuropeptides (e.g.,  
383 oxytocin, vasopressin, or somatostatin) in brain circuits and behavior has been particularly  
384 challenging due to the lack of specific methods for localized uncaging or release (DeLaney et  
385 al., 2018). While several caged neuropeptides have been reported, their application *in vivo* is  
386 limited by instability due to peptidase degradation (Ma et al., 2023; Xiong et al., 2023b). An  
387 alternative approach involves targeting neurons that endogenously produce these  
388 neuropeptides using cre-recombinase and expressing opsins to either opto-stimulate or inhibit  
389 the neuron and the subsequent neuropeptide release (Arrigoni and Saper, 2014; Dao et al.,  
390 2019). However, a major limitation of this approach is that neuropeptides are often co-released  
391 with classical neurotransmitters (Merighi, 2002; Hökfelt et al., 2003), making it challenging to  
392 isolate and study their specific functions.

393 A new technology based on photosensitive nanovesicles has been developed to address  
394 these limitations. Photosensitive nanovesicles encapsulate neuroactive molecules in self-  
395 assembled nanoscale vesicles, such as those made by a bilayer of phospholipids (liposomes)  
396 and a light-sensitive component for the photosensitive release. This innovative approach  
397 addresses the limitations of traditional pharmacology and provides a versatile platform to  
398 decipher the role of neuropeptides and neuromodulators. Specifically, the physical separation of  
399 neuroactive molecules from the surrounding brain environment improves *in vivo* stability  
400 compared with caged compounds.

401 Plasmonic gold-coated nanovesicles, in combination with Cell-based Neurotransmitter  
402 Fluorescent Engineered Reporter (PACE), have been used to investigate neuropeptide  
403 signaling in the mouse neocortex *in vivo* (Fig. 6A,B) (Xiong et al., 2022). Near-infrared light  
404 stimulation triggered the release of femtoliters to picoliters of Somatostatin-14 (SST) from  
405 nanovesicles in the brain, which was subsequently detected by activation of SST2 CNiFERs

406 tuned to nanomolar concentrations of SST. PACE revealed a reduced yet coordinated SST  
407 transmission within 130  $\mu$ m, with significantly diminished and delayed transmission at greater  
408 distances. PACE provides a novel method for examining the scale and timing of neuropeptide  
409 volume transmission and signaling within the brain.

410 Another class of photosensitive nanovesicles involves photoswitchable azobenzenes.  
411 Azobenzene groups have gained significant attention in the field of photoswitches (Bahamonde  
412 et al., 2014; Cabré et al., 2019; Morstein et al., 2019, 2020, 2022; DiFrancesco et al., 2020;  
413 Kellner and Berlin, 2020; Mukhopadhyay et al., 2022). These compounds exhibit reversible  
414 trans-cis photoisomerization. Recently, researchers incorporated azobenzene into lipids by  
415 replacing one of the hydrophobic tails on the phospholipid, leading to the development of  
416 photoswitchable lipids, including the photoswitchable phosphatidylcholine derivative azo-PC  
417 (Pernpeintner et al., 2017; Urban et al., 2018, 2020; Pritzl et al., 2020, 2022). Azo-PC enables  
418 optical control of membrane organization and permeability, providing a versatile framework for  
419 delivering neuroactive compounds. Building upon the concept of photoswitchable lipids, a new  
420 class of photoswitchable nanovesicles termed “azosomes” have been developed. Azosomes  
421 consist of liposomes formulated with azo-PC. When the azobenzene undergoes reversible  
422 isomerization, it increases the permeability of the membrane and allows the contents to diffuse  
423 out (**Fig. 6C-E**). Computational studies suggest that trans-configuration may decrease the  
424 thickness of the lipid bilayer, thereby increasing permeability for encapsulated molecules.<sup>109</sup> The  
425 ability to switch the release of molecules on and off using short light pulses (< 3 seconds)  
426 demonstrates the potential of azosomes for neuromodulation. Recently, azosomes loaded with  
427 the D1 agonist SKF-81297 were shown to modulate striatal neurons *in vitro* upon light  
428 stimulation (Xiong et al., 2023a).

429 To explore the utility of azosomes *in vivo*, they are being tested in awake, behaving mice  
430 using fiber photometry to control the release of agonists and simultaneously monitor neural  
431 activity. For control, calcein-azosomes were infused into one hemisphere and calcein-liposomes  
432 (non-photoswitchable) into the opposite hemisphere. A dual optic fiber delivered light stimulation  
433 and monitored fluorescence on both hemispheres. The hemisphere implanted with calcein-  
434 azosomes (but not calcein-liposomes) exhibited a fluorescence increase upon light photo-  
435 switching, confirming the photo-release of calcein *in vivo*. To study the photo-release of SKF-  
436 81297 from azosomes *in vivo*, D1-medium spiny neurons (MSNs) in the dorsomedial striatum, a  
437 region involved in locomotor activity control, were targeted. While monitoring D1-MSN Ca<sup>2+</sup>  
438 dynamics (with DIO GCaMP expressed in a D1-Cre mouse) and the distance traveled, it is  
439 possible to simultaneously photo-release an azosome’s cargo, record neuronal activity, and  
440 monitor motor behavior. Additionally, we are exploring the use of azosomes to release  
441 neuropeptides, expanding the repertoire of neuroactive compounds that can be remotely  
442 released.

443 In summary, photosensitive nanovesicles possess several features that make them  
444 promising tools for the controlled release of neuroactive compounds and precise  
445 neuromodulation. Photosensitive nanovesicles can be loaded with fluorescent dyes, drugs, or  
446 neuropeptides, allowing for versatile applications. Harnessing the ability to remotely and  
447 precisely control the release of neuroactive compounds *in vivo* will further elucidate the *in vivo*  
448 function of several neuropeptides in the future.

449 **Conclusions:**

450 Revealing the brain’s intricacy, with its expansive neural network, synaptic connections,  
451 and fine-tuned genetic and biochemical regulations, remains challenging. Details at the cellular  
452 and molecular levels and their control of cognitive function remain especially elusive. However,  
453 this gap is continuously narrowing thanks to transgenic model organisms and techniques like  
454 fluorescence imaging, CRISPR/Cas9 gene editing, protein tickertapes, and time-locked release  
455 of neuromodulators, allowing real-time *in vivo* functional circuit mapping. Notably, using protein-

457 based tools in genetically-defined neuronal subpopulations has illuminated the granular control  
458 of circuit function by a diverse array of cell types and neuromodulators. Concurrent  
459 advancements in imaging, epitomized by head-mounted Miniscopes, promise deeper insights  
460 into previously inaccessible brain regions. New fluorescent sensors, especially for  
461 neuropeptides, are of high priority to maximize the synergistic effects of these developments.  
462 Emerging high-throughput techniques for sensor optimization, combined with machine learning,  
463 are ideally suited to expedite advancements. Additionally, the revolutionary CRISPR/Cas9 gene  
464 editing techniques are increasingly used *in vivo* to delineate the genetic underpinnings of brain  
465 function, while photosensitive nanovesicles promise increased precision in neuromodulation.  
466 One major challenge for the future is overcoming the tradeoff between spatial and temporal  
467 information. *In vivo* imaging, electrophysiology, and fiber photometry enable dynamic yet  
468 spatially restricted monitoring, while *ex vivo* imaging can provide spatially expansive yet  
469 primarily static information. Collectively, the emerging tools and methodologies highlighted in  
470 this review are elucidating the brain's functional architecture and outlining future innovations in  
471 circuit mapping.

472

473

474

## 475 **References**

476 Abraham AD, Casello SM, Schattauer SS, Wong BA, Mizuno GO, Mahe K, Tian L, Land BB,  
477 Chavkin C (2021) Release of endogenous dynorphin opioids in the prefrontal cortex  
478 disrupts cognition. *Neuropsychopharmacology* 46:2330–2339.

479 Adam Y et al. (2019) Voltage imaging and optogenetics reveal behaviour-dependent changes in  
480 hippocampal dynamics. *Nature* 569:413–417 Available at: <https://doi.org/10.1038/s41586-019-1166-7>.

482 Airan RD, Meyer RA, Ellens NPK, Rhodes KR, Farahani K, Pomper MG, Kadam SD, Green JJ  
483 (2017) Noninvasive Targeted Transcranial Neuromodulation via Focused Ultrasound Gated  
484 Drug Release from Nanoemulsions. *Nano Lett* 17:652–659 Available at:  
485 <https://doi.org/10.1021/acs.nanolett.6b03517>.

486 Andermann ML, Gilfoy NB, Goldey GJ, Sachdev RNS, Wölfel M, McCormick DA, Reid RC,  
487 Levene MJ (2013) Chronic cellular imaging of entire cortical columns in awake mice  
488 using microprisms. *Neuron* 80:900–913.

489 Arrigoni E, Saper CB (2014) What optogenetic stimulation is telling us (and failing to tell us)  
490 about fast neurotransmitters and neuromodulators in brain circuits for wake-sleep  
491 regulation. *Curr Opin Neurobiol* 0:165 Available at: /pmc/articles/PMC4268002/ [Accessed  
492 August 22, 2023].

493 Bahamonde MI, Taura J, Paoletta S, Gakh AA, Chakraborty S, Hernando J, Fernández-Dueñas  
494 V, Jacobson KA, Gorostiza P, Ciruela F (2014) Photomodulation of G Protein-Coupled  
495 Adenosine Receptors by a Novel Light-Switchable Ligand. *Bioconjug Chem* 25:1847–1854  
496 Available at: <https://doi.org/10.1021/bc5003373>.

497 Cabré G, Garrido-Charles A, Moreno M, Bosch M, Porta-de-la-Riva M, Krieg M, Gascón-Moya  
498 M, Camarero N, Gelabert R, Lluch JM, Busqué F, Hernando J, Gorostiza P, Alibés R  
499 (2019) Rationally designed azobenzene photoswitches for efficient two-photon neuronal  
500 excitation. *Nat Commun* 10:907 Available at: <https://doi.org/10.1038/s41467-019-08796-9>.

501 Cai DJ et al. (2016) A shared neural ensemble links distinct contextual memories encoded close  
502 in time. *Nature* 534:115–118 Available at: <https://doi.org/10.1038/nature17955>.

503 Charpentier E, Marraffini LA (2014) Harnessing CRISPR-Cas9 immunity for genetic  
504 engineering. *Curr Opin Microbiol* 19:114–119 Available at:  
505 <https://pubmed.ncbi.nlm.nih.gov/25048165/> [Accessed July 20, 2023].

506 Chen T-W, Wardill TJ, Sun Y, Pulver SR, Renninger SL, Baohan A, Schreiter ER, Kerr RA,  
507 Orger MB, Jayaraman V, Looger LL, Svoboda K, Kim DS (2013) Ultra-sensitive fluorescent  
508 proteins for imaging neuronal activity. *Nature* 499:295 Available at:  
509 [/pmc/articles/PMC3777791/](https://pmc/articles/PMC3777791/) [Accessed October 4, 2021].

510 Choi EY, Franco D, Stafp CA, Gordin M, Chow A, Cover KK, Chandra R, Kay Lobo M (2023)  
511 Inducible CRISPR Epigenome Systems Mimic Cocaine Induced Bidirectional Regulation of  
512 Nab2 and Egr3. *J Neurosci* 43:2242–2259 Available at:  
513 <https://pubmed.ncbi.nlm.nih.gov/36849419/> [Accessed July 20, 2023].

514 Choudhury SR, Cui Y, Lubecka K, Stefanska B, Irudayaraj J (2016) CRISPR-dCas9 mediated  
515 TET1 targeting for selective DNA demethylation at BRCA1 promoter. *Oncotarget* 7:46545–  
516 46556 Available at: <https://pubmed.ncbi.nlm.nih.gov/27356740/> [Accessed July 20, 2023].

517 Copits BA et al. (2021) A photoswitchable GPCR-based opsin for presynaptic inhibition. *Neuron*  
518 109:1791-1809.e11 Available at: <https://doi.org/10.1016/j.neuron.2021.04.026>.

519 Cox DBT, Platt RJ, Zhang F (2015) Therapeutic genome editing: prospects and challenges. *Nat  
520 Med* 21:121–131 Available at: <https://pubmed.ncbi.nlm.nih.gov/25654603/> [Accessed July  
521 20, 2023].

522 Dao NC, Brockway DF, Crowley NA (2019) In Vitro Optogenetic Characterization of  
523 Neuropeptide Release from Prefrontal Cortical Somatostatin Neurons. *Neuroscience*  
524 419:1–4 Available at: <http://www.ncbi.nlm.nih.gov/article/S0306452219305706/fulltext>  
525 [Accessed August 22, 2023].

526 Day JJ (2019) Genetic and epigenetic editing in nervous system. *Dialogues Clin Neurosci*  
527 21:359–368 Available at: <https://pubmed.ncbi.nlm.nih.gov/31949403/> [Accessed July 20,  
528 2023].

529 de Groot A, van den Boom BJJ, van Genderen RM, Coppens J, van Veldhuijzen J, Bos J,  
530 Hoedemaker H, Negrello M, Willuhn I, De Zeeuw CI, Hoogland TM (2020) NINscope, a  
531 versatile miniscope for multi-region circuit investigations Carey MR, Wassum KM, Cai DJ,  
532 eds. *Elife* 9:e49987 Available at: <https://doi.org/10.7554/eLife.49987>.

533 DeLaney K, Buchberger AR, Atkinson L, Gründer S, Mousley A, Li L (2018) New techniques,  
534 applications and perspectives in neuropeptide research. *J Exp Biol* 221 Available at:  
535 [/pmc/articles/PMC5818036/](https://pmc/articles/PMC5818036/) [Accessed August 22, 2023].

536 DiFrancesco ML et al. (2020) Neuronal firing modulation by a membrane-targeted photoswitch.  
537 *Nat Nanotechnol* 15:296–306 Available at: <https://doi.org/10.1038/s41565-019-0632-6>.

538 Dong Z, Mau W, Feng Y, Pennington ZT, Chen L, Zaki Y, Rajan K, Shuman T, Aharoni D, Cai  
539 DJ (2022) Minian, an open-source miniscope analysis pipeline Kemere C, Colgin LL,  
540 Kemere C, eds. *Elife* 11:e70661 Available at: <https://doi.org/10.7554/eLife.70661>.

541 Duffet L et al. (2022) A genetically encoded sensor for in vivo imaging of orexin neuropeptides.  
542 Nat Methods 19:231–241 Available at: <https://doi.org/10.1038/s41592-021-01390-2>.

543 Duke CG, Bach S V., Revanna JS, Sultan FA, Southern NT, Davis MN, Carullo NVN, Bauman  
544 AJ, Phillips RA, Day JJ (2020) An Improved CRISPR/dCas9 Interference Tool for Neuronal  
545 Gene Suppression. Front Genome Ed 2:9 Available at: [/pmc/articles/PMC8525373/](https://PMC8525373/)  
546 [Accessed July 20, 2023].

547 Ellis-Davies GCR (2007) Caged compounds: photorelease technology for control of cellular  
548 chemistry and physiology. Nat Methods 4:619–628 Available at:  
549 <https://doi.org/10.1038/nmeth1072>.

550 Ellis-Davies GCR (2020) Useful Caged Compounds for Cell Physiology. Acc Chem Res  
551 53:1593–1604 Available at: <https://doi.org/10.1021/acs.accounts.0c00292>.

552 Feng J, Zhang C, Lischinsky JE, Jing M, Zhou J, Wang H, Zhang Y, Dong A, Wu Z, Wu H, Chen  
553 W, Zhang P, Zou J, Hires SA, Zhu JJ, Cui G, Lin D, Du J, Li Y (2019) A Genetically  
554 Encoded Fluorescent Sensor for Rapid and Specific In Vivo Detection of Norepinephrine.  
555 Neuron 102:745–761.e8 Available at:  
556 <http://www.sciencedirect.com/science/article/pii/S0896627319301722>.

557 Fosque BF, Sun Y, Dana H, Yang CT, Ohyama T, Tadross MR, Patel R, Zlatic M, Kim DS,  
558 Ahrens MB, Jayaraman V, Looger LL, Schreiter ER (2015) Neural circuits. Labeling of  
559 active neural circuits in vivo with designed calcium integrators. Science (New York, NY)  
560 347:755–760.

561 Ghosh KK, Burns LD, Cocker ED, Nimmerjahn A, Ziv Y, Gamal A El, Schnitzer MJ (2011)  
562 Miniaturized integration of a fluorescence microscope. Nat Methods 8:871 Available at:  
563 [/pmc/articles/PMC3810311/](https://PMC3810311/) [Accessed October 4, 2021].

564 Gilbert LA, Larson MH, Morsut L, Liu Z, Brar GA, Torres SE, Stern-Ginossar N, Brandman O,  
565 Whitehead EH, Doudna JA, Lim WA, Weissman JS, Qi LS (2013) CRISPR-mediated  
566 modular RNA-guided regulation of transcription in eukaryotes. Cell 154:442–451.

567 Giovannucci A, Friedrich J, Gunn P, Kalfon J, Brown BL, Koay SA, Taxidis J, Najafi F, Gauthier  
568 JL, Zhou P, Khakh BS, Tank DW, Chklovskii DB, Pnevmatikakis EA (2019) CalmAn an  
569 open source tool for scalable calcium imaging data analysis Kleinfeld D, King AJ, eds. Elife  
570 8:e38173 Available at: <https://doi.org/10.7554/eLife.38173>.

571 Glaser A et al. (2023) Expansion-assisted selective plane illumination microscopy for nanoscale  
572 imaging of centimeter-scale tissues. bioRxiv:2023.06.08.544277 Available at:  
573 <http://biorxiv.org/content/early/2023/06/27/2023.06.08.544277.abstract>.

574 Gong S, Doughty M, Harbaugh CR, Cummins A, Hatten ME, Heintz N, Gerfen CR (2007)  
575 Targeting Cre recombinase to specific neuron populations with bacterial artificial  
576 chromosome constructs. J Neurosci 27:9817–9823.

577 Gunaydin LA, Grosenick L, Finkelstein JC, Kauvar IV, Fenno LE, Adhikari A, Lammel S,  
578 Mirzabekov JJ, Airan RD, Zalocusky KA, Tye KM, Anikeeva P, Malenka RC, Deisseroth K  
579 (2014) Natural Neural Projection Dynamics Underlying Social Behavior. Cell 157:1535–  
580 1551 Available at:  
581 <http://www.ncbi.nlm.nih.gov/pubmed/24949967%0Ahttp://www.ncbi.nlm.nih.gov/article>

582 erender.fcgi?artid=PMC4123133%0Ahttp://linkinghub.elsevier.com/retrieve/pii/S009286741  
583 400659X.

584 Heidenreich M, Zhang F (2016) Applications of CRISPR-Cas systems in neuroscience. *Nat Rev  
585 Neurosci* 17:36–44 Available at: <https://pubmed.ncbi.nlm.nih.gov/26656253/> [Accessed  
586 July 20, 2023].

587 Hökfelt T, Bartfai T, Bloom F (2003) Neuropeptides: opportunities for drug discovery. *Lancet  
588 Neurol* 2:463–472 Available at:  
589 <http://www.thelancet.com/article/S1474442203004824/fulltext> [Accessed August 22, 2023].

590 Hunker AC, Soden ME, Krayushkina D, Heymann G, Awatramani R, Zweifel LS (2020)  
591 Conditional Single Vector CRISPR/SaCas9 Viruses for Efficient Mutagenesis in the Adult  
592 Mouse Nervous System. *Cell Rep* 30:4303-4316.e6 Available at:  
593 <https://pubmed.ncbi.nlm.nih.gov/32209486/> [Accessed July 20, 2023].

594 Hyun JH, Nagahama K, Namkung H, Mignocchi N, Roh SE, Hannan P, Krüssel S, Kwak C,  
595 McElroy A, Liu B, Cui M, Lee S, Lee D, Huganir RL, Worley PF, Sawa A, Kwon HB (2022)  
596 Tagging active neurons by soma-targeted Cal-Light. *Nature communications* 13.

597 Jiang F, Doudna JA (2017) CRISPR-Cas9 Structures and Mechanisms. *Annu Rev Biophys*  
598 46:505–529 Available at: <https://pubmed.ncbi.nlm.nih.gov/28375731/> [Accessed July 20,  
599 2023].

600 Jing M et al. (2020) An optimized acetylcholine sensor for monitoring in vivo cholinergic activity.  
601 *Nat Methods* 17:1139 Available at: [/pmc/articles/PMC7606762/](https://pmc/articles/PMC7606762/) [Accessed October 4,  
602 2021].

603 Josselyn SA, Tonegawa S (2020) Memory engrams: Recalling the past and imagining the  
604 future. *Science* 367.

605 Juarez B, Kong M-S, Jo YS, Elum JE, Yee JX, Ng-Evans S, Cline M, Hunker AC, Quinlan MA,  
606 Baird MA, Elerding AJ, Johnson M, Ban D, Mendez A, Goodwin NL, Soden ME, Zweifel LS  
607 (2023) Temporal scaling of dopamine neuron firing and dopamine release by distinct ion  
608 channels shape behavior. *Sci Adv* 9:eadg8869 Available at:  
609 <https://doi.org/10.1126/sciadv.adg8869>.

610 Juneau J, Duret G, Chu JP, Rodriguez A V, Morozov S, Aharoni D, Robinson JT, St-Pierre F,  
611 Kemere C (2020) MiniFAST: A sensitive and fast miniaturized microscope for &lt;em&gt;in  
612 vivo&lt;/em&gt; neural recording. *bioRxiv*:2020.11.03.367466 Available at:  
613 <http://biorxiv.org/content/early/2020/11/05/2020.11.03.367466.abstract>.

614 Kalamakis G, Platt RJ (2023) CRISPR for neuroscientists. *Neuron* Available at:  
615 <https://pubmed.ncbi.nlm.nih.gov/37201524/> [Accessed July 20, 2023].

616 Kellner S, Berlin S (2020) Two-Photon Excitation of Azobenzene Photoswitches for Synthetic  
617 Optogenetics. *Applied Sciences* 10 Available at: [https://www.mdpi.com/2076-3417/10/3/805](https://www.mdpi.com/2076-<br/>618 3417/10/3/805).

619 Kim CK, Sanchez MI, Hoerbelt P, Fenno LE, Malenka RC, Deisseroth K, Ting AY (2020) A  
620 Molecular Calcium Integrator Reveals a Striatal Cell Type Driving Aversion. *Cell* 183:2003–  
621 2019.e16.

622 Kim D, Park P, Li X, Campos JDW, Tian H, Moult EM, Grimm JB, Lavis L, Cohen AE (2023)  
623 Mapping memories: pulse-chase labeling reveals AMPA receptor dynamics during memory  
624 formation. *bioRxiv*.

625 Kim MW, Wang W, Sanchez MI, Coukos R, von Zastrow M, Ting AY (2017) Time-gated  
626 detection of protein-protein interactions with transcriptional readout. *eLife* 6.

627 Koveal D, Rosen PC, Meyer DJ, Díaz-García CM, Wang Y, Cai L-H, Chou PJ, Weitz DA, Yellen  
628 G (2022) A high-throughput multiparameter screen for accelerated development and  
629 optimization of soluble genetically encoded fluorescent biosensors. *Nat Commun* 13:2919  
630 Available at: <https://doi.org/10.1038/s41467-022-30685-x>.

631 Lee D, Creed M, Jung K, Stefanelli T, Wendler DJ, Oh WC, Mignocchi NL, Lüscher C, Kwon HB  
632 (2017a) Temporally precise labeling and control of neuromodulatory circuits in the  
633 mammalian brain. *Nature Methods* 2017 14:5 14:495–503.

634 Lee D, Hyun JH, Jung K, Hannan P, Kwon HB (2017b) A calcium- and light-gated switch to  
635 induce gene expression in activated neurons. *Nature biotechnology* 35:858–863.

636 Levene MJ, Dombeck DA, Kasischke KA, Molloy RP, Webb WW (2004) In vivo multiphoton  
637 microscopy of deep brain tissue. United States.

638 Limaye A, Hall B, Kulkarni AB (2009) Manipulation of Mouse Embryonic Stem Cells for  
639 Knockout Mouse Production. *Current protocols in cell biology / editorial board, Juan S*  
640 *Bonifacino . [et al]* CHAPTER:Unit Available at: [/pmc/articles/PMC2759096/](https://pmc/articles/PMC2759096/) [Accessed July  
641 20, 2023].

642 Lin D, Li X, Moult E, Park P, Tang B, Shen H, Grimm JB, Falco N, Jia BZ, Baker D, Lavis LD,  
643 Cohen AE (2023) Time-tagged ticker tapes for intracellular recordings. *Nature*  
644 *biotechnology* 41:631–639.

645 Liu Q, Zhang Z, Zhang W (2021) Optogenetic Dissection of Neural Circuits Underlying Stress-  
646 Induced Mood Disorders. *Front Psychol* 12 Available at:  
647 <https://www.frontiersin.org/articles/10.3389/fpsyg.2021.600999>.

648 Ma X, Johnson DA, He XJ, Layden AE, McClain SP, Yung JC, Rizzo A, Bonaventura J,  
649 Banghart MR (2023) In vivo photopharmacology with a caged mu opioid receptor agonist  
650 drives rapid changes in behavior. *Nat Methods* 20:682–685 Available at:  
651 <https://doi.org/10.1038/s41592-023-01819-w>.

652 Mahn M et al. (2021) Efficient optogenetic silencing of neurotransmitter release with a  
653 mosquito rhodopsin. *Neuron* 109:1621-1635.e8.

654 Maier W, Corrie JET, Papageorgiou G, Laube B, Grewer C (2005) Comparative analysis of  
655 inhibitory effects of caged ligands for the NMDA receptor. *J Neurosci Methods* 142:1–9.

656 Mathis A, Mamidanna P, Cury KM, Abe T, Murthy VN, Mathis MW, Bethge M (2018)  
657 DeepLabCut: markerless pose estimation of user-defined body parts with deep learning.  
658 *Nat Neurosci* 21:1281–1289 Available at: <https://doi.org/10.1038/s41593-018-0209-y>.

659 McQuillan HJ, Clarkson J, Kauff A, Han SY, Yip SH, Cheong I, Porteous R, Heather AK,  
660 Herbison AE (2022) Definition of the estrogen negative feedback pathway controlling the

661 GnRH pulse generator in female mice. *Nat Commun* 13 Available at:  
662 <https://pubmed.ncbi.nlm.nih.gov/36460649/> [Accessed July 20, 2023].

663 Merighi A (2002) Costorage and coexistence of neuropeptides in the mammalian CNS. *Prog*  
664 *Neurobiol* 66:161–190.

665 Mohar B, Grimm JB, Patel R, Brown TA, Tillberg P, Lavis LD, Spruston N, Svoboda K (2022)  
666 Brain-wide measurement of protein turnover with high spatial and temporal resolution.  
667 *bioRxiv*:2022.11.12.516226.

668 Morstein J, Dacheux MA, Norman DD, Shemet A, Donthamsetti PC, Citir M, Frank JA, Schultz  
669 C, Isacoff EY, Parrill AL, Tigyi GJ, Trauner D (2020) Optical Control of Lysophosphatidic  
670 Acid Signaling. *J Am Chem Soc* 142:10612–10616 Available at:  
671 <https://doi.org/10.1021/jacs.0c02154>.

672 Morstein J, Hill RZ, Novak AJE, Feng S, Norman DD, Donthamsetti PC, Frank JA, Harayama T,  
673 Williams BM, Parrill AL, Tigyi GJ, Riezman H, Isacoff EY, Bautista DM, Trauner D (2019)  
674 Optical control of sphingosine-1-phosphate formation and function. *Nat Chem Biol* 15:623–  
675 631 Available at: <https://doi.org/10.1038/s41589-019-0269-7>.

676 Morstein J, Romano G, Hetzler BE, Plante A, Haake C, Levitz J, Trauner D (2022)  
677 Photoswitchable Serotonins for Optical Control of the 5-HT2A. *Angew Chem Int Ed Engl*  
678 61:e202117094 Available at: [/pmc/articles/PMC9423688/](https://pmc/articles/PMC9423688/) [Accessed August 22, 2023].

679 Mukhopadhyay TK, Morstein J, Trauner D (2022) Photopharmacological control of cell signaling  
680 with photoswitchable lipids. *Curr Opin Pharmacol* 63:102202 Available at:  
681 <https://www.sciencedirect.com/science/article/pii/S147148922000297>.

682 Noguchi J, Nagaoka A, Watanabe S, Ellis-Davies GCR, Kitamura K, Kano M, Matsuzaki M,  
683 Kasai H (2011) In vivo two-photon uncaging of glutamate revealing the structure–function  
684 relationships of dendritic spines in the neocortex of adult mice. *J Physiol* 589:2447  
685 Available at: [/pmc/articles/PMC3115818/](https://pmc/articles/PMC3115818/) [Accessed August 22, 2023].

686 Oh SW et al. (2014) A mesoscale connectome of the mouse brain. *Nature* 508:207–214  
687 Available at: <https://doi.org/10.1038/nature13186>.

688 Parker JG, Marshall JD, Ahanonu B, Wu Y-W, Kim TH, Grewe BF, Zhang Y, Li JZ, Ding JB,  
689 Ehlers MD, Schnitzer MJ (2018) Diametric neural ensemble dynamics in parkinsonian and  
690 dyskinetic states. *Nature* 557:177–182 Available at: <https://doi.org/10.1038/s41586-018-0090-6>.

692 Patriarchi T, Cho JR, Merten K, Howe MW, Marley A, Xiong W-H, Folk RW, Broussard GJ,  
693 Liang R, Jang MJ, Zhong H, Dombeck D, von Zastrow M, Nimmerjahn A, Gradinaru V,  
694 Williams JT, Tian L (2018) Ultrafast neuronal imaging of dopamine dynamics with designed  
695 genetically encoded sensors. *Science* (1979) Available at:  
696 <http://science.sciencemag.org/content/early/2018/05/30/science.aat4422.abstract>.

697 Pernpeintner C, Frank JA, Urban P, Roeske CR, Pritzl SD, Trauner D, Lohmüller T (2017) Light-  
698 Controlled Membrane Mechanics and Shape Transitions of Photoswitchable Lipid Vesicles.  
699 *Langmuir* 33:4083–4089 Available at: <https://doi.org/10.1021/acs.langmuir.7b01020>.

700 Pickar-Oliver A, Gersbach CA (2019) The next generation of CRISPR-Cas technologies and  
701 applications. *Nat Rev Mol Cell Biol* 20:490–507 Available at:  
702 <https://pubmed.ncbi.nlm.nih.gov/31147612/> [Accessed July 20, 2023].

703 Platt RJ et al. (2014) CRISPR-Cas9 knockin mice for genome editing and cancer modeling. *Cell*  
704 159:440–455 Available at: <https://pubmed.ncbi.nlm.nih.gov/25263330/> [Accessed July 20,  
705 2023].

706 Pritzl SD, Konrad DB, Ober MF, Richter AF, Frank JA, Nickel B, Trauner D, Lohmüller T (2022)  
707 Optical Membrane Control with Red Light Enabled by Red-Shifted Photolipids. *Langmuir*  
708 38:385–393 Available at: <https://doi.org/10.1021/acs.langmuir.1c02745>.

709 Pritzl SD, Urban P, Prasselsperger A, Konrad DB, Frank JA, Trauner D, Lohmüller T (2020)  
710 Photolipid Bilayer Permeability is Controlled by Transient Pore Formation. *Langmuir*  
711 36:13509–13515 Available at: <https://doi.org/10.1021/acs.langmuir.0c02229>.

712 Rao S, Chen R, LaRocca AA, Christiansen MG, Senko AW, Shi CH, Chiang P-H, Varnavides G,  
713 Xue J, Zhou Y, Park S, Ding R, Moon J, Feng G, Anikeeva P (2019) Remotely controlled  
714 chemomagnetic modulation of targeted neural circuits. *Nat Nanotechnol* 14:967–973  
715 Available at: <https://doi.org/10.1038/s41565-019-0521-z>.

716 Rapp TL, DeForest CA (2021) Targeting Drug Delivery with Light: A Highly Focused Approach.  
717 *Adv Drug Deliv Rev* 171:94 Available at: [/pmc/articles/PMC8127392/](https://pmc/articles/PMC8127392/) [Accessed August 22,  
718 2023].

719 Rappleye M, Gordon-Fennel A, Castro D, Matarasso A, Zamorano C, Wait S, Lee J, Siebart J,  
720 Suko A, Smith N, Muster J, Matreyek K, Fowler D, Stuber G, Bruchas M, Berndt A (2022)  
721 Opto-MASS: a high-throughput engineering platform for genetically encoded fluorescent  
722 sensors enabling all optical *in vivo* detection of monoamines and neuropeptides. *BioRxiv*.

723 Rynes ML, Surinach DA, Linn S, Laroque M, Rajendran V, Dominguez J, Hadjistamoulou O,  
724 Navabi ZS, Ghanbari L, Johnson GW, Nazari M, Mohajerani MH, Kodandaramaiah SB  
725 (2021) Miniaturized head-mounted microscope for whole-cortex mesoscale imaging in  
726 freely behaving mice. *Nat Methods* 18:417–425.

727 Sanchez MI, Nguyen QA, Wang W, Soltesz I, Ting AY (2020) Transcriptional readout of  
728 neuronal activity via an engineered Ca<sup>2+</sup>-activated protease. *Proceedings of the National*  
729 *Academy of Sciences of the United States of America* 117:33186–33196.

730 Savell KE, Bach S V., Zipperly ME, Revanna JS, Goska NA, Tuscher JJ, Duke CG, Sultan FA,  
731 Burke JN, Williams D, Ianov L, Day JJ (2019) A Neuron-Optimized CRISPR/dCas9  
732 Activation System for Robust and Specific Gene Regulation. *eNeuro* 6 Available at:  
733 <https://pubmed.ncbi.nlm.nih.gov/30863790/> [Accessed July 20, 2023].

734 Savell KE, Day JJ (2017) Focus: Genome Editing: Applications of CRISPR/Cas9 in the  
735 Mammalian Central Nervous System. *Yale J Biol Med* 90:567 Available at:  
736 [/pmc/articles/PMC5733858/](https://pmc/articles/PMC5733858/) [Accessed July 20, 2023].

737 Scholefield J, Harrison PT (2021) Prime editing – an update on the field. *Gene Ther* 28:396  
738 Available at: [/pmc/articles/PMC8376635/](https://pmc/articles/PMC8376635/) [Accessed July 20, 2023].

739 Scott BB, Thiberge SY, Guo C, Tervo DGR, Brody CD, Karpova AY, Tank DW (2018) Imaging  
740 Cortical Dynamics in GCaMP Transgenic Rats with a Head-Mounted  
741 Widefield Microscope. *Neuron* 100:1045-1058.e5.

742 Silva JM, Silva E, Reis RL (2019) Light-triggered release of photocaged therapeutics - Where  
743 are we now? *Journal of Controlled Release* 298:154–176.

744 Soden ME, Yee JX, Zweifel LS (2023) Circuit coordination of opposing neuropeptide and  
745 neurotransmitter signals. *Nature* 619 Available at:  
746 <https://pubmed.ncbi.nlm.nih.gov/37380765/> [Accessed July 20, 2023].

747 Stierl M, Stumpf P, Udwari D, Gueta R, Hagedorn R, Losi A, Gärtnér W, Petereit L, Efetova M,  
748 Schwarzel M, Oertner TG, Nagel G, Hegemann P (2011) Light modulation of cellular cAMP  
749 by a small bacterial photoactivated adenylyl cyclase, bPAC, of the soil bacterium  
750 *Beggiatoa*. *Journal of Biological Chemistry* 286:1181–1188 Available at:  
751 <http://www.jbc.org/article/S0021925820563060/fulltext> [Accessed August 22, 2023].

752 Swiech L, Heidenreich M, Banerjee A, Habib N, Li Y, Trombetta J, Sur M, Zhang F (2015) In  
753 vivo interrogation of gene function in the mammalian brain using CRISPR-Cas9. *Nat*  
754 *Biotechnol* 33:102–106 Available at: <https://pubmed.ncbi.nlm.nih.gov/25326897/> [Accessed  
755 July 20, 2023].

756 Taura J, Nolen EG, Cabré G, Hernando J, Squarcialupi L, López-Cano M, Jacobson KA,  
757 Fernández-Dueñas V, Ciruela F (2018) Remote control of movement disorders using a  
758 photoactive adenosine A2A receptor antagonist. *J Control Release* 283:135 Available at:  
759 [/pmc/articles/PMC6098950/](https://pmc/articles/PMC6098950/) [Accessed August 22, 2023].

760 Tian H, Davis HC, Wong-Campos JD, Park P, Fan LZ, Gmeiner B, Begum S, Werley CA, Borja  
761 GB, Upadhyay H, Shah H, Jacques J, Qi Y, Parot V, Deisseroth K, Cohen AE (2023)  
762 Video-based pooled screening yields improved far-red genetically encoded voltage  
763 indicators. *Nat Methods* 20:1082–1094 Available at: <https://doi.org/10.1038/s41592-022-01743-5>.

765 Urban P, Pritzl SD, Konrad DB, Frank JA, Pernpeintner C, Roeske CR, Trauner D, Lohmüller T  
766 (2018) Light-Controlled Lipid Interaction and Membrane Organization in Photolipid Bilayer  
767 Vesicles. *Langmuir* 34:13368–13374 Available at:  
768 <https://doi.org/10.1021/acs.langmuir.8b03241>.

769 Urban P, Pritzl SD, Ober MF, Dirscherl CF, Pernpeintner C, Konrad DB, Frank JA, Trauner D,  
770 Nickel B, Lohmueller T (2020) A Lipid Photoswitch Controls Fluidity in Supported Bilayer  
771 Membranes. *Langmuir* 36:2629–2634 Available at:  
772 <https://doi.org/10.1021/acs.langmuir.9b02942>.

773 Urnov FD, Miller JC, Lee YL, Beausejour CM, Rock JM, Augustus S, Jamieson AC, Porteus  
774 MH, Gregory PD, Holmes MC (2005) Highly efficient endogenous human gene correction  
775 using designed zinc-finger nucleases. *Nature* 435:646–651 Available at:  
776 <https://pubmed.ncbi.nlm.nih.gov/15806097/> [Accessed July 20, 2023].

777 Vardy E et al. (2015) A New DREADD Facilitates the Multiplexed Chemogenetic Interrogation of  
778 Behavior. *Neuron* 86:936–946 Available at: <http://dx.doi.org/10.1016/j.neuron.2015.03.065>.

779 Venkatachalam V, Brinks D, Maclaurin D, Hochbaum D, Kralj J, Cohen AE (2014) Flash  
780 Memory: Photochemical Imprinting of Neuronal Action Potentials onto a Microbial  
781 Rhodopsin. *Journal of the American Chemical Society* 136:2529.

782 Wait SJ, Rappleye M, Lee JD, Smith N, Berndt A (2023) Machine Learning Ensemble Directed  
783 Engineering of Genetically Encoded Fluorescent Calcium Indicators.  
784 bioRxiv:2023.04.13.536801.

785 Wang H, Yang H, Shivalila CS, Dawlaty MM, Cheng AW, Zhang F, Jaenisch R (2013) One-Step  
786 Generation of Mice Carrying Mutations in Multiple Genes by CRISPR/Cas-Mediated  
787 Genome Engineering. *Cell* 153:910 Available at: [/pmc/articles/PMC3969854/](https://pmc/articles/PMC3969854/) [Accessed  
788 July 20, 2023].

789 Wang JB, Aryal M, Zhong Q, Vyas DB, Airan RD (2018) Noninvasive Ultrasonic Drug Uncaging  
790 Maps Whole-Brain Functional Networks. *Neuron* 100:728-738.e7 Available at:  
791 <https://www.sciencedirect.com/science/article/pii/S0896627318309504>.

792 Wang Y, Wang M, Yin S, Jang R, Wang J, Xue Z, Xu T (2015) NeuroPep: a comprehensive  
793 resource of neuropeptides. *Database* 2015:bav038 Available at:  
794 <https://doi.org/10.1093/database/bav038>.

795 Weinholtz CA, Castle MJ (2021) Intersectional targeting of defined neural circuits by adeno-  
796 associated virus vectors. *J Neurosci Res* 99:981–990.

797 Wirtshafter HS, Disterhoft JF (2022) In Vivo Multi-Day Calcium Imaging of CA1 Hippocampus in  
798 Freely Moving Rats Reveals a High Preponderance of Place Cells with Consistent Place  
799 Fields. *J Neurosci* 42:4538–4554.

800 Xiong H, Alberto KA, Youn J, Taura J, Morstein J, Li X, Wang Y, Trauner D, Slesinger PA,  
801 Nielsen SO, Qin Z (2023a) Optical control of neuronal activities with photoswitchable  
802 nanovesicles. *Nano Res* 16:1033–1041 Available at: <https://doi.org/10.1007/s12274-022-4853-x>.

803 Xiong H, Lacin E, Ouyang H, Naik A, Xu X, Xie C, Youn J, Wilson BA, Kumar K, Kern T,  
804 Aisenberg E, Kircher D, Li X, Zasadzinski JA, Mateo C, Kleinfeld D, Hrabetova S, Slesinger  
805 PA, Qin Z (2022) Probing Neuropeptide Volume Transmission In Vivo by Simultaneous  
806 Near-Infrared Light-Triggered Release and Optical Sensing\*\*. *Angewandte Chemie*  
807 International Edition 61:e202206122 Available at: <https://doi.org/10.1002/anie.202206122>.

808 Xiong H, Wilson BA, Slesinger PA, Qin Z (2023b) Understanding Neuropeptide Transmission in  
809 the Brain by Optical Uncaging and Release. *ACS Chem Neurosci* 14:516–523 Available at:  
810 <https://doi.org/10.1021/acschemneuro.2c00684>.

811 Yamaguchi H, Hopf FW, Li S Bin, de Lecea L (2018) In vivo cell type-specific CRISPR  
812 knockdown of dopamine beta hydroxylase reduces locus coeruleus evoked wakefulness.  
813 *Nat Commun* 9 Available at: <https://pubmed.ncbi.nlm.nih.gov/30523254/> [Accessed July  
814 20, 2023].

815 Yanny K, Antipa N, Liberti W, Dehaeck S, Monakhova K, Liu FL, Shen K, Ng R, Waller L (2020)  
816 Miniscope3D: optimized single-shot miniature 3D fluorescence microscopy. *Light Sci Appl*  
817 9:171 Available at: <https://doi.org/10.1038/s41377-020-00403-7>.

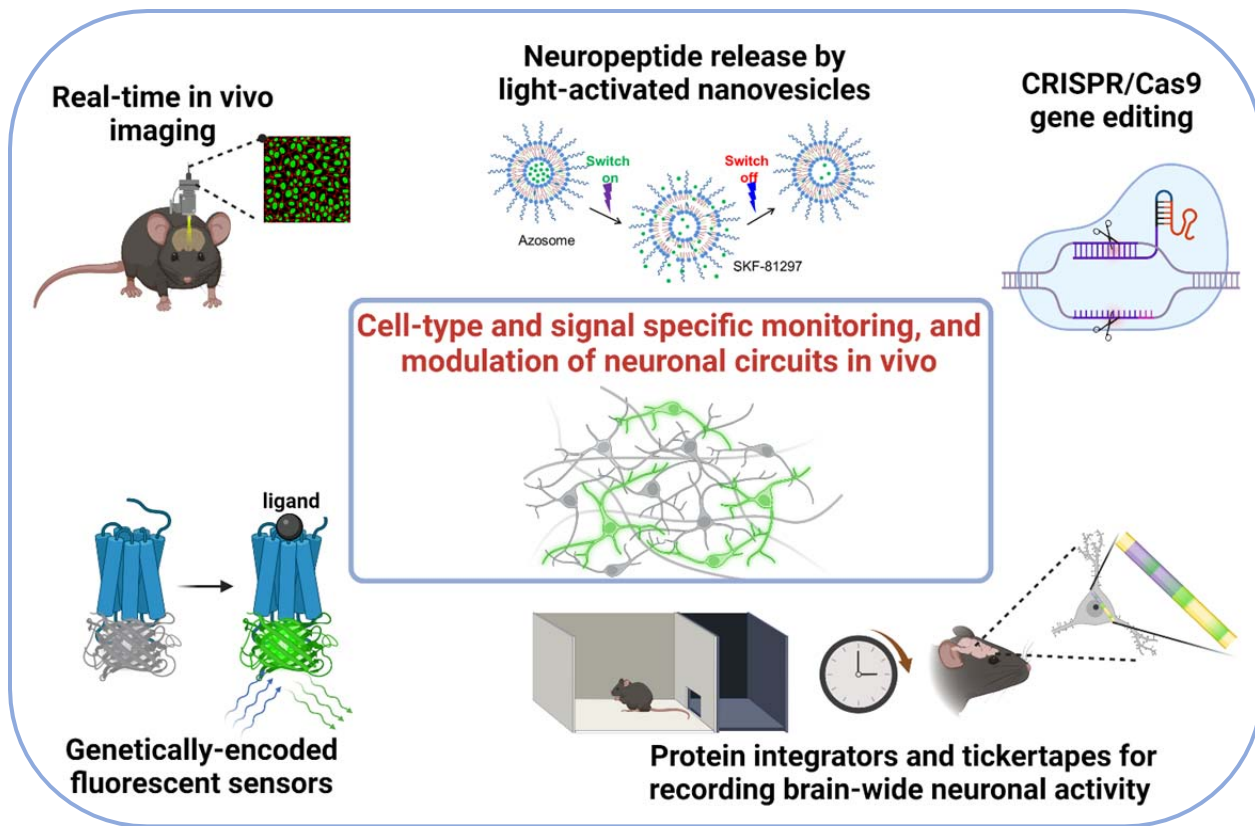
819 Yizhar O, Fenno LE, Davidson TJ, Mogri M, Deisseroth K (2011) Optogenetics in neural  
820 systems. *Neuron* 71:9–34.

821 Zaki Y, Pennington ZT, Morales-Rodriguez D, Francisco TR, LaBanca AR, Dong Z, Segura SC,  
822 Silva AJ, Shuman T, Fenton A, Rajan K, Cai DJ (2023) Aversive experience drives offline  
823 ensemble reactivation to link memories across days. *bioRxiv*:2023.03.13.532469 Available  
824 at: <http://biorxiv.org/content/early/2023/03/14/2023.03.13.532469.abstract>.

825 Zhang Y et al. (2023) Fast and sensitive GCaMP calcium indicators for imaging neural  
826 populations. *Nature* 615:884–891 Available at: <https://doi.org/10.1038/s41586-023-05828-9>.

828 Zong W, Wu R, Chen S, Wu J, Wang H, Zhao Z, Chen G, Tu R, Wu D, Hu Y, Xu Y, Wang Y,  
829 Duan Z, Wu H, Zhang Y, Zhang J, Wang A, Chen L, Cheng H (2021) Miniature two-photon  
830 microscopy for enlarged field-of-view, multi-plane and long-term brain imaging. *Nature*  
831 *Methods* 2021 18:1 18:46–49 Available at: <https://www.nature.com/articles/s41592-020-01024-z> [Accessed August 22, 2023].

833  
834  
835  
836  
837  
838  
839  
840  
841  
842  
843  
844  
845  
846  
847  
848  
849  
850  
851  
852  
853



854

855 **Figure 1.** Comprehensive *in vivo* circuit mapping requires the modulations and monitoring of  
 856 genetically defined neuron populations. This review highlights recent advances in techniques to  
 857 study neuronal circuits on the genetic, molecular, and cellular levels. Applying these methods *in*  
 858 *vivo* could link circuit functions to cognitive processes and disease mechanisms. (Figure created  
 859 with BioRender.com)

860

861

862

863

864

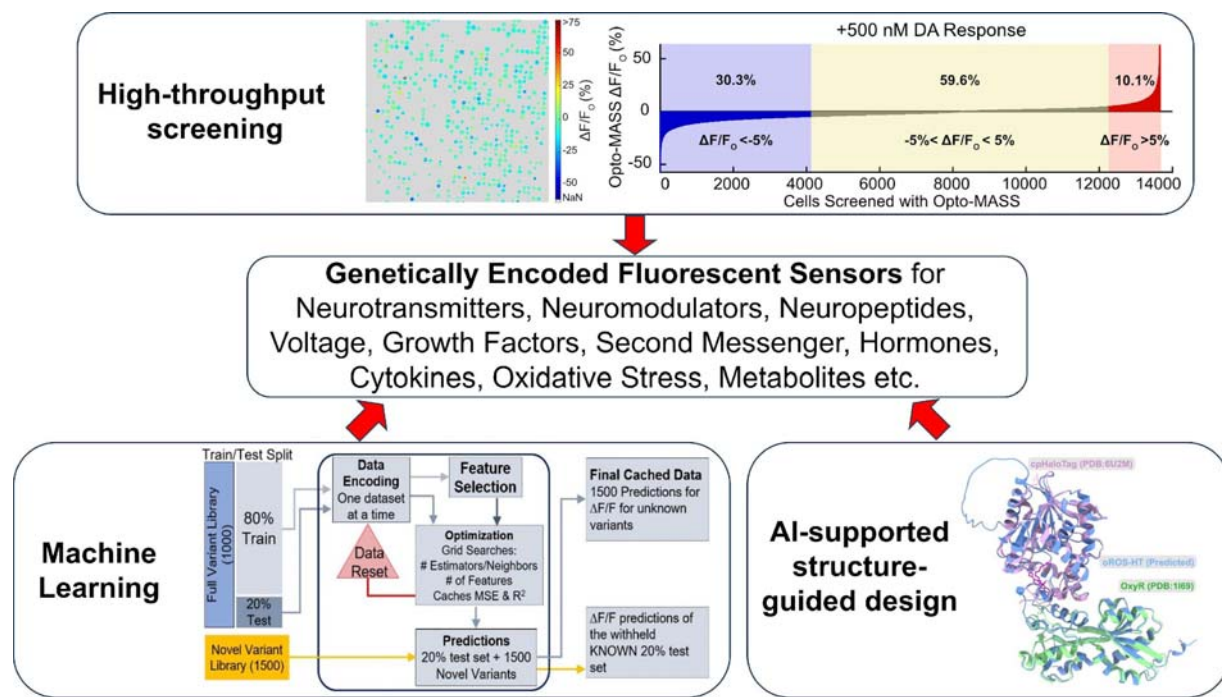
865

866

867

868

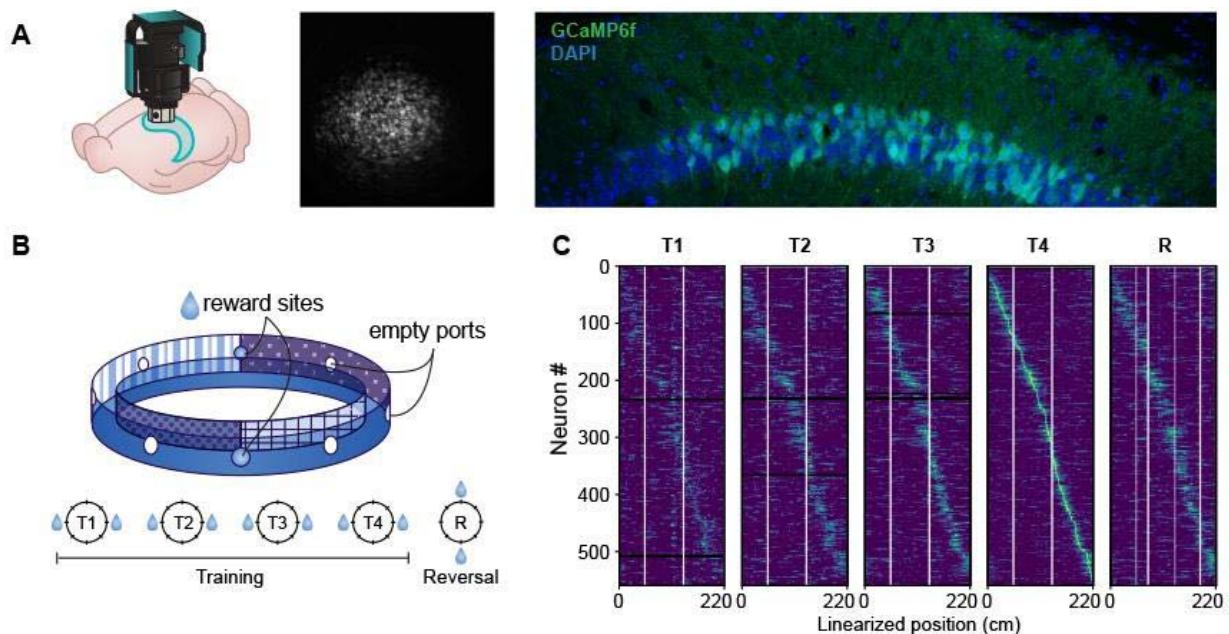
869



871 **Figure 2. Next-generation approaches for engineering genetically encoded fluorescent**  
 872 **sensors.** Thousands of biological compounds regulate brain activities and cognitive functions.  
 873 Fluorescent protein sensors for these compounds can be designed following similar design  
 874 principles. However, optimizing dynamic range, signal sensitivity, and kinetics is hampered by  
 875 the immense mutational space of each sensor protein. Therefore, further advancements in  
 876 protein engineering are required by integrating high-throughput functional testing of large variant  
 877 libraries, data-driven approaches, and AI-supported structure-guided design. The figure has  
 878 been adapted from (Rappleye et al., 2022; Wait et al., 2023) with permission.

879  
 880  
 881  
 882  
 883  
 884  
 885  
 886  
 887  
 888  
 889

890



891

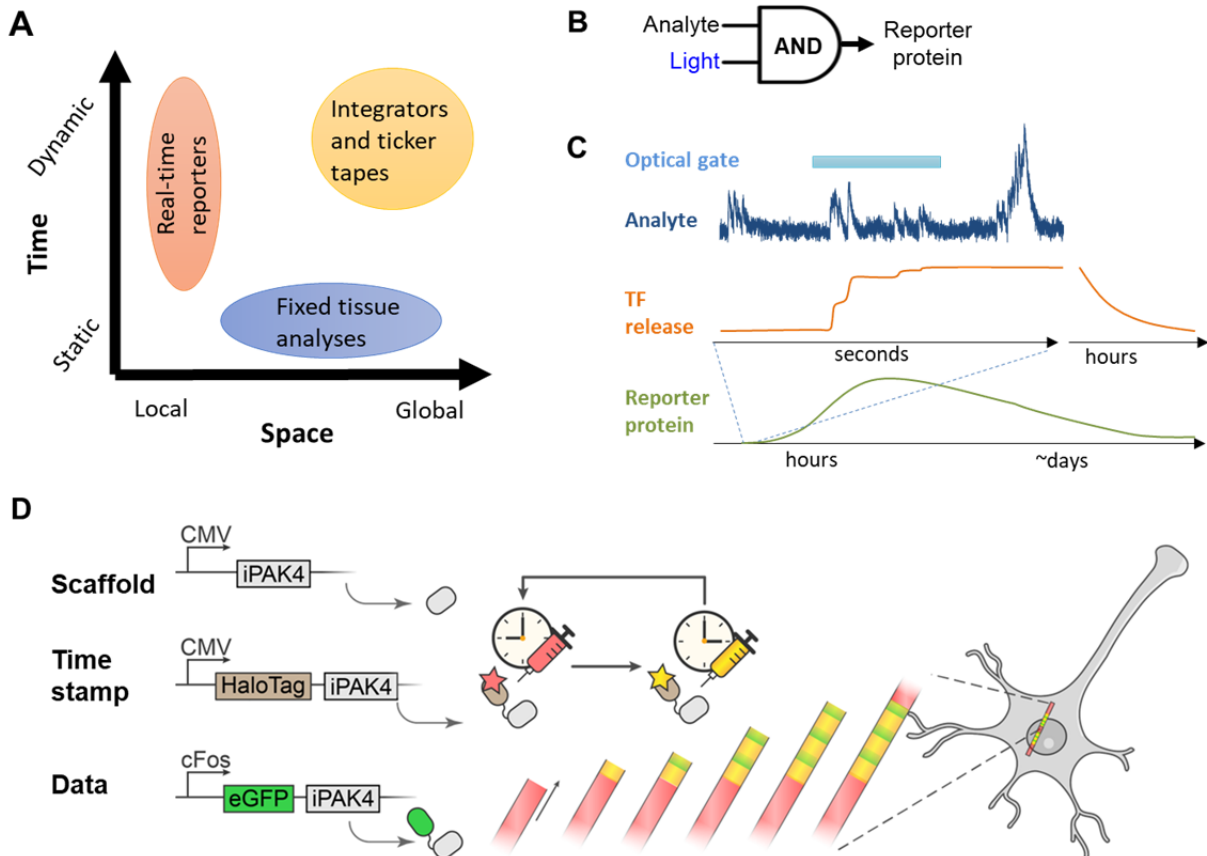
892 **Figure 3. A.** Technologies such as Miniscope calcium imaging allow real-time observations of  
893 neuronal ensembles *in vivo*. while mice perform behavioral tasks **(B)**. **C.** Computational analysis  
894 of the imaging sessions allows to identify the dynamic activity of hundreds of neurons.

895

896

897

898



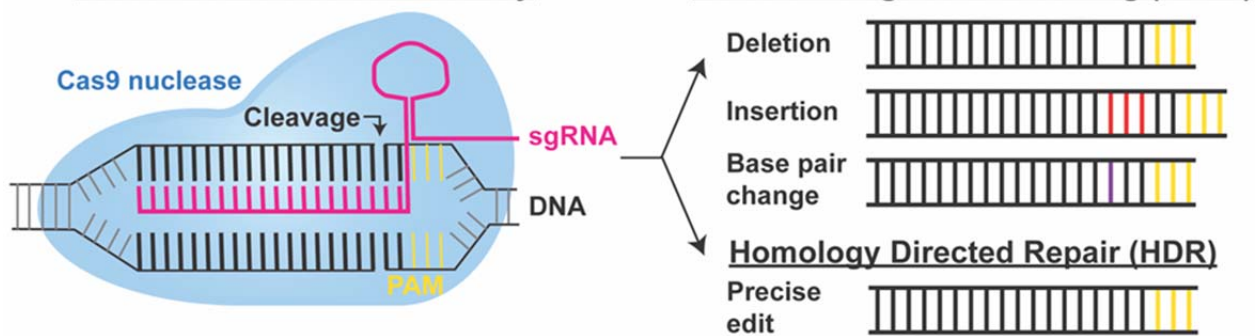
899  
900  
901  
902

903 **Figure 4. Integrators and tickertapes transcend the tradeoffs between *in vivo* and *ex vivo***  
904 **imaging.** A. Real-time reporters probe neural dynamics but with a limited field of view; *ex vivo*  
905 analyses can access the whole brain but provide static snapshots. Integrators and tickertapes  
906 can provide dynamic, brain-wide information. B. Light-gated integrators convert the cumulative  
907 level of an analyte during an illumination epoch into a transcriptional readout. C. Schematic  
908 operation of a light-gated integrator. Dynamic fluctuations in an analyte (e.g.,  $\text{Ca}^{2+}$ ) are  
909 converted into transcription factor (TF) release during an illumination epoch. The TF drives  
910 expression of a reporter protein. D. Example tickertape recorder. A linearly growing scaffold is  
911 marked at periodic intervals via alternating injection of two colors of HaloTag-ligand dye. An  
912 activity-dependent promoter (e.g., cFos) drives expression of a GFP-labeled monomer which  
913 introduces green stripes into the fiber. Localization of the green stripes relative to the red/yellow  
914 color transitions identifies the timing of neural activity. Figure (D) was adapted with permission  
915 from (Lin et al., 2023)

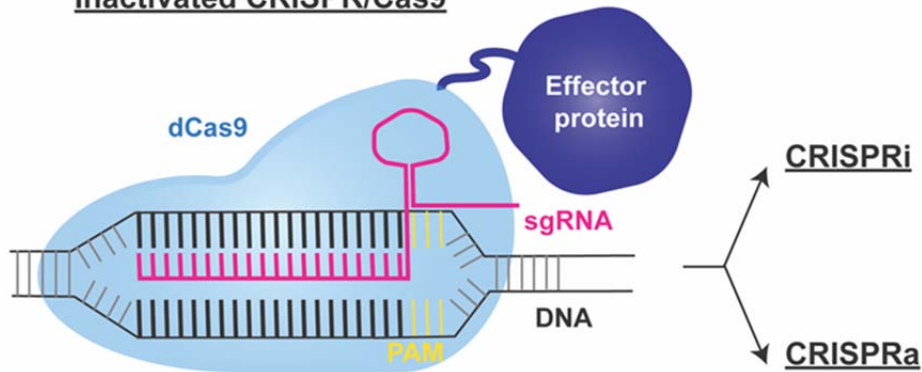
916  
917  
918  
919  
920  
921  
922  
923  
924

925

**A. CRISPR/Cas9 nuclease activity**



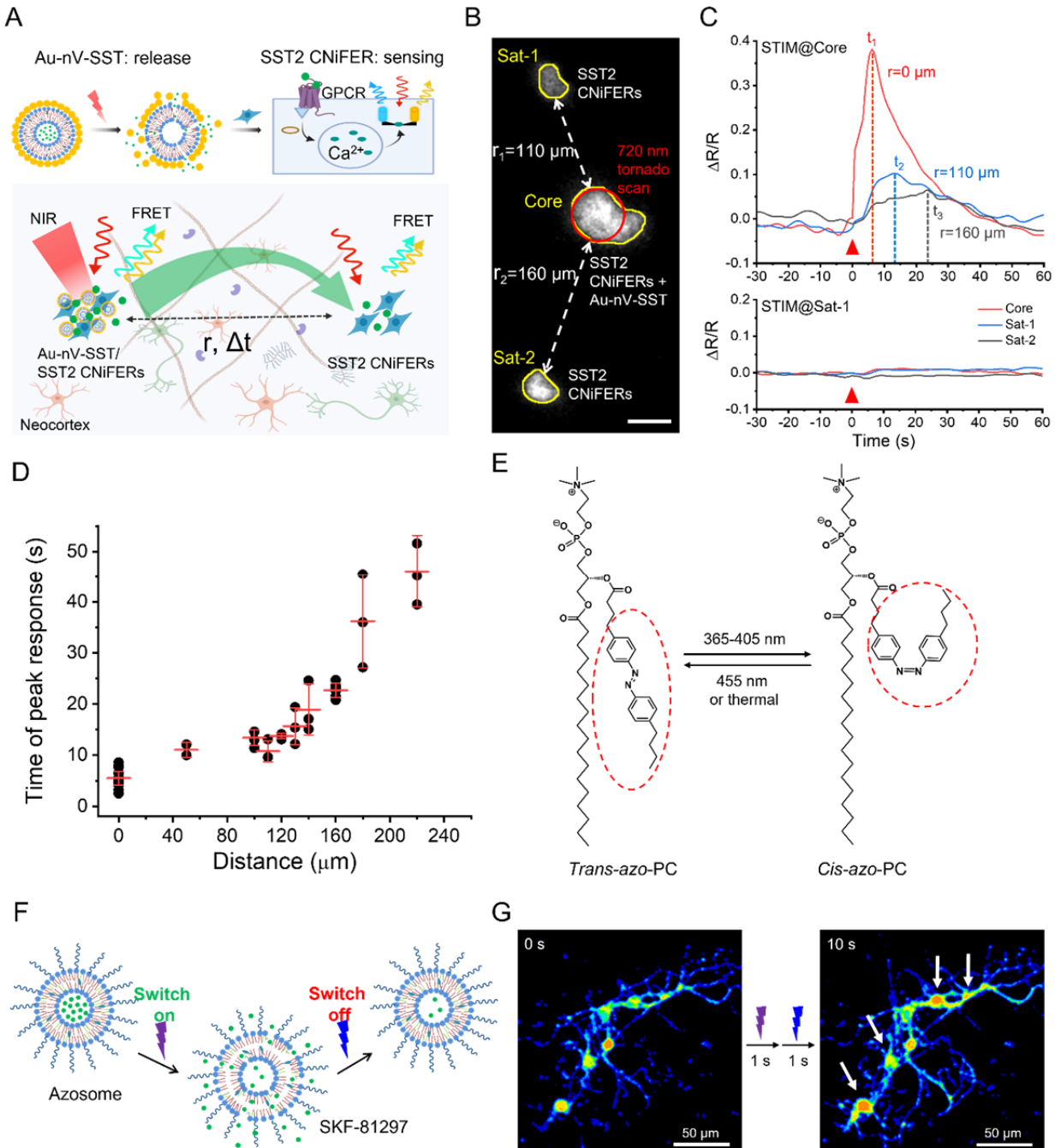
**B. Inactivated CRISPR/Cas9**



926  
927  
928  
929  
930

**Figure 5. Capabilities of the CRISPR/Cas9 toolbox. A.** Systems using CRISPR/Cas9 components with Cas9's nuclease activity intact will cause DNA cleavage and error-prone NHEJ, most likely employed in neurons or precise editing with HDR. **B.** CRISPR/Cas9 systems with inactive nuclease activity, or dCas9, can be fused with effector proteins to further modify gene expression.

936  
937



938

939 **Figure 6. Photosensitive nanovesicles for precise neuromodulation.**

940 **A.** Schematic of neuropeptide transmission measurement by plasmonic gold-coated

941 nanovesicles (Au-nV-SST) and two clusters of SST2 CNiFERs. **B.** Two-photon fluorescent

942 image of SST2 CNiFERs at 200μm in the mouse cortex. (Ex: 900 nm; Em: 520-560 nm). **C.**

943 Response curves for SST2 CNiFERs when stimulated (STIM) at different regions (core vs

944 satellite 1/sat-1). **D.** Peak response time of SST2 CNiFER implants at defined distances from

945 the core implant. **E.** Schematic of the photoisomerization of azo-PC. **F.** Schematic of the

946 photoswitchable release of SKF-81297 from azosome. **G** Real-time fluorescent images of

947 cultured primary mouse striatal neurons before and after the irradiation of sequential 365 nm

948 light and 455 nm light. Fluo-4 was used as the Ca<sup>2+</sup> indicator. Scale bar: 50 μm. Figures

949 (A,B,C) were adapted with permission from [95]. Figures (D,E,F) were adapted with permission  
950 from (Xiong et al., 2023).